Noninvasive Identification of Atrial Fibrillation Drivers: Simulation and Patient Data Evaluation

Maria S Guillem[1], Andreu M Climent[2], Miguel Rodrigo[1], Ismael Hernández-Romero[2,3], Alejandro Liberos[1,2], Francisco Fernández-Avilés[2,4], Omer Berenfeld[5], Felipe Atienza[2,4]

[1]ITACA, Universitat Politècnica de Valencia, Valencia, Spain
[2]Cardiology Department, Hospital General Universitario Gregorio Marañón, Instituto de Investigación Sanitaria Gregorio Marañón, Madrid, Spain
[3]Department of Telecommunication Engineering, Universidad Rey Juan Carlos, Fuenlabrada, Spain
[4]Facultad de Medicina, Universidad Complutense de Madrid, Madrid, Spain
[5]Center for Arrhythmia Research, University of Michigan, Ann Arbor, MI, USA

Abstract

Identification of atrial drivers as singularity points by using the inverse problem of electrocardiography is being used to guide atrial fibrillation (AF) ablation. However, the ability of the inverse problem to reconstruct fibrillation patterns and identify AF drivers has not been validated.

Position of AF drivers was compared between recorded and inverse computed EGMs by making use of (1) realistic mathematical models and (2) simultaneous endocardial and body surface recordings during AF ablation procedures. Atrial drivers were defined as the areas with the highest dominant frequencies (HDF) or at the sites with a higher incidence of long-lasting phase singularities (PS).

On simulation data, HDF analysis allowed the identification of the chamber that harboured the AF source in 30 out of 30 of the models evaluated vs. 26 out of 30 models for PS analysis. On patient data, solution of the inverse problem only allowed identifying atrial drivers on the correct atrial chamber by HDF analysis (2 out of 2 patients vs. 0 out of 2 patients for PS analysis).

Identification of atrial sources by solving the inverse problem of the electrocardiography is more reliably accomplished based HDF than on PS detection.

1. Introduction

Atrial fibrillation (AF) is the most frequent arrhythmia encountered in the clinical practice, and is associated with multiple co-morbidities. In spite of its high prevalence, the treatment for AF is suboptimal, with reported success rates of around 70% [1]

Pulmonary vein isolation (PVI) has been established as the recommended catheter ablation approach with overall success rates of up to 87% in paroxysmal AF patients [2]. However, success rates of catheter ablation in non-paroxysmal AF patients are disappointing, with AF-free rates for single a procedure as low as 28% [3].

Recently, different alternatives have been proposed based on a personalized identification of the mechanisms responsible for AF by making use of electrical mapping, which can either be invasive, by intracavitary catheters [4] or noninvasive, by using surface recordings and resolution of the inverse problem of electrocardiography [5], both with promising success rates which are especially relevant on non-paroxysmal AF patients. However, most electrophysiologists are skeptical regarding these inverse computed potentials because the activation patterns they report are way simpler than epicardial maps recorded both by electrical or optical mapping during AF.

In order to clarify the relation between noninvasive mapping recordings and intracardiac AF activity, we compared driver identifications based on highest dominant frequencies and on phase sinpularities of both invasive and inverse-computed electrograms by making use of mathematical simulations and patient data.

2. Materials and methods

2.1. Computational models of the atria and torso

A realistic 3D model of the atrial anatomy composed by 284,578 nodes and 1,353,783 tetrahedrons (673.4±130.3 μm between nodes) was used to simulate the atrial electrical activity [6]. A gradient on the electrophysiological properties of the atrial myocardium, specifically on $I_{k,ACh}$, I_{K1}, I_{Na} and I_{CaL} was introduced into

the atrial cell formulation [7,8] to obtain propagation patterns maintained by rotors and with spatial variations in the activation rate. Fibrotic tissue was modeled by disconnecting an amount of nodes between 20% and 60% of total, and scar tissue by disconnecting 100% of nodes in the scar region. The system of differential equations in the atrial cell model was solved by using Runge-Kutta integration based on a graphic processors unit (NVIDIA Tesla C2075 6G) [9].

An ensemble of 30 different AF episodes was simulated, composed of 14 AF patterns driven by a single rotor at varying locations of the LA (PVs, PLAW and LAA) and 16 AF patterns driven by a single rotor at varying locations of the RA (free RA wall and RAA).

For each simulation, a uniform mesh of unipolar EGMs was calculated surrounding the epicardial surface (1 mm distance) under the assumption of a homogenous, unbounded and quasi-static conducting medium by summing up all effective dipole contributions over the entire model [10]. Computed electrograms were stored for processing at a sampling frequency of 500 Hz.

The ECG potentials on the torso model were calculated by solving the Forward Problem with the Boundary Element Method in a mesh formed by 771 nodes and 1538 triangular patches, with electrical conductivities used were 3S/m for blood and 2S/m for tissue [11].

2.2. Simultaneous body surface and intracardiac recordings in AF patients

Two patients admitted for ablation of drug-refractory paroxysmal AF were studied. The ablation protocol as previously described was approved by the Institutional Ethics Committee of our institution and both patients gave informed consent. Patients arrived in sinus rhythm and AF was induced using electrical burst pacing.

In order to reconstruct the electrical activity on the heart surface by solving the inverse problem of the electrocardiography, body surface potential mapping (BSPM) technique was used whereby multichannel electrocardiograms (ECGs) were recorded. A total of 57 chest ECG leads were recorded using a commercial system (ClearsignTM Amplifier, Boston Scientific, Natick, MA) and the electrodes were distributed as follows: 24 electrodes on the anterior, 24 on the posterior, 3 on each lateral side of the torso and 3 extra leads in order to obtain a Wilson Central Terminal. The geometry of the atria and torso of each patient was obtained by segmentation of computed axial tomography (CAT) images. Specifically, images with a spatial resolution of 0.5 mm were acquired prior to the ablation procedure and segmented by using 3D Slicer.

Body surface recordings were obtained simultaneously with a 64-pole basket catheter (Constellation, Boston Scientific, Natick, MA, USA) located sequentially on the right and left atria. Additionally, a standard tetrapolar catheter was placed in the coronary sinus (CS) and a 20-pole catheter in the opposite atrium to the basket catheter. With the basket catheter located inside each atrium, a central bolus of adenosine (12–18 mg) was administered.

2.3. Inverse problem resolution

We estimated the inverse-computed EGM (iEGM) from both patient recordings and mathematical models by computing the inverse of the field transfer atrial-torso matrix by using zero-order Tikhonov's. The optimal regularization parameter was chosen according to the L-curve method.

2.4. Identification of AF drivers

AF drivers were identified in electrophysiological signals based on both spectral analysis and phase mapping.

For spectral analysis, signals were band-pass filtered between 2 and 30 Hz as previously described [13]. Power spectral density of all signals was computed using Welch's periodogram (65536 point Fast Fourier transform and 80% overlap) to determine the local DFs with a spectral resolution of 0.01Hz [12]. AF drivers were defined as the center of mass of the region with the highest DF (HDF).

Rotor location was carried out by identification of singularity points (SP) in the phase map obtained with the Hilbert Transform [13]. Phase values were obtained along 3 different circles surrounding each evaluated point, and six to twelve points per circle were used for the phase analysis in which the signal was interpolated by a weighted average of the neighboring nodes, being d-2 the weight for each node and d the distance between nodes.

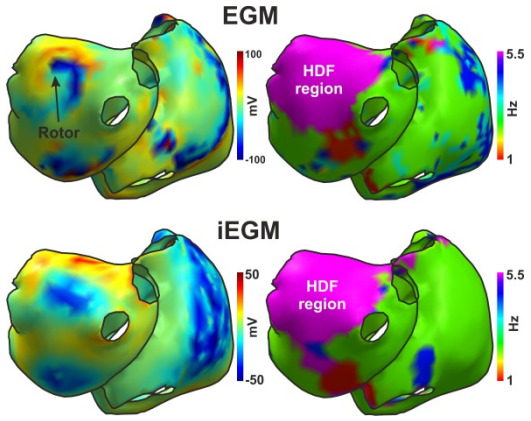

Figure 1. DF maps of a sample mathematical model with a high frequency rotor on the PV region. Top: modelled EGMs. Bottom: inverse-computed EGMs.

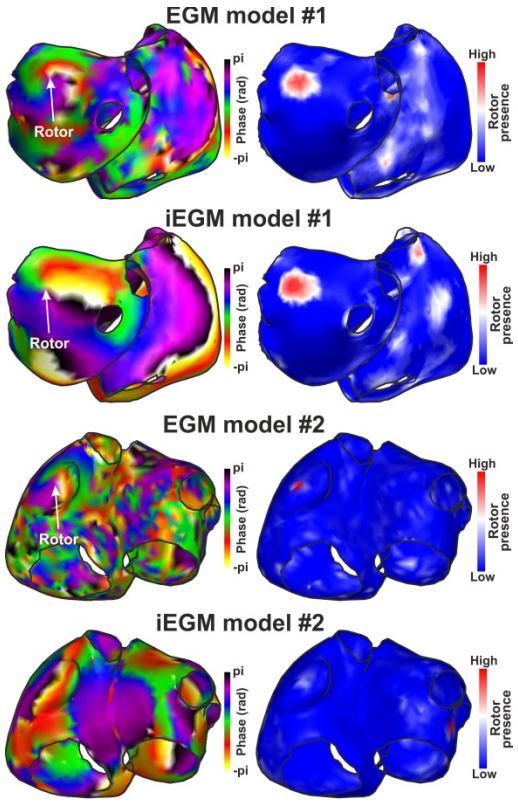

Figure 2. Phase maps and PS incidence in two sample mathematical models. For each model on top: modelled EGMs and bottom: inverse-computed.

An evaluated point was defined as a SP only when the phases of at least two of these three circles was monotonically increasing or decreasing for a total of 2π. A rotor was defined as the connection between SPs across time. The distance between SPs at consecutive time instants should be less than 1 cm (EGM and iEGM) or 5 cm (ECG) to be related and maintain a continuity of rotation. Finally, only long lasting rotors, defined as those that complete at least one rotation were considered as rotors and other SPs were discarded.

3. Results

3.1. AF driver identification in models

On simulation data, HDF analysis allowed the identification of the chamber with the AF source in 30 out of 30 of the models evaluated. As it can be observed in the sample case of Fig 1, DF maps are not identical, but both HDF regions are placed in the same atrial region, the pulmonary vein region, which harboured a high frequency rotor.

As it can be observed in Fig 2, inverse-computed phase maps are simpler than those of the models, but still allowed rotor identification in 26 out of 30 cases, but some rotors were not accurately located, such as model#2.

3.2. AF driver identification in patients

In patients, solution of the inverse problem allowed identifying atrial drivers on the correct atrial chamber (RA) by HDF analysis in both patients, as it can be observed in Fig 3.

In these patients, the highest incidence of PS was inscribed inside the HDF area for the actual EGMs recorded by the multipolar catheter baskets, as it can be observed in Fig 4. However, sites of highest PS incidence did not match between recorded and inverse-computed EGMs. Indeed incidence of rotors was higher in the opposed atrial chamber (LA) for both patients based on inverse-computed EGMs.

4. Discussion

We have recently shown that inverse-computed EGMs are poorly related to contact electrograms, with large relative errors in the instantaneous phase [11]. In this work, we have demonstrated that reconstruction errors can be mostly attributed to a loss of complexity, quantified in terms of the number of simultaneous phase singularities. This loss of complexity is consistent with a mutual cancellation of propagation wavefronts with opposed directions [10] that may not be retrievable by solving the inverse problem.

Despite this loss of information at the body surface level, surface potentials have shown to keep some relevant attributes of AF drivers both in terms of their activation frequency [12] and rotor location [11].

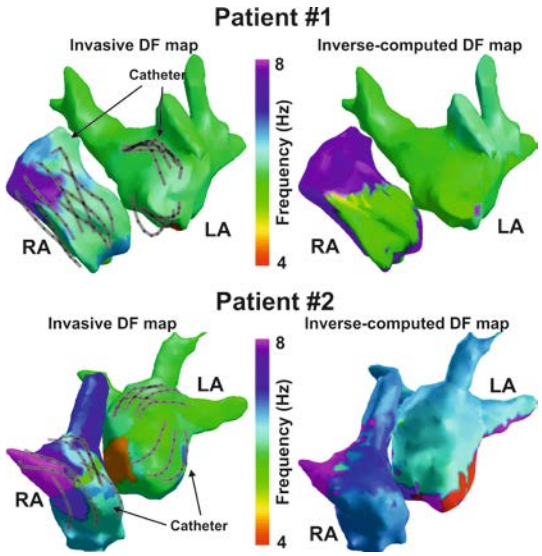

Figure 3. DF maps of two AF patients. For each patient, on the right: DF map obtained from basket catheters; on the left, DF map obtained from iEGMs.

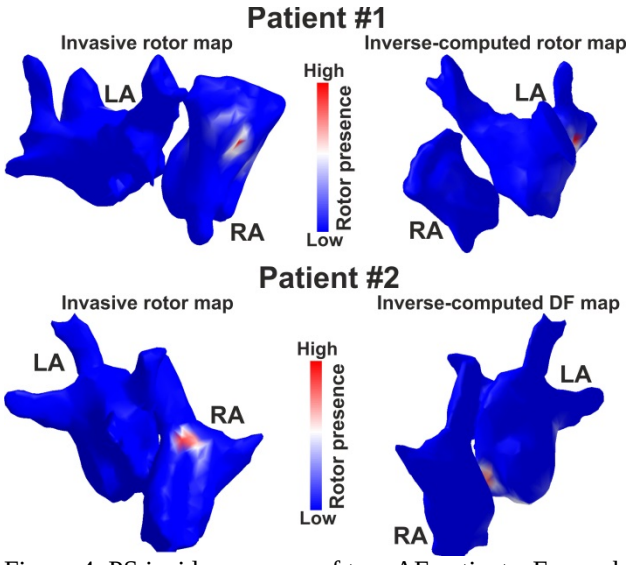

Figure 4. PS incidence maps of two AF patients. For each patient, on the right: PS map obtained from basket catheters; on the left, PS map obtained from iEGMs.

Here we have shown that activation-based parameters, such as the activation frequency computed by spectral analysis or rotor location computed by applying phase transform, are quite robust against both signal and model uncertainties in our modelling data. However, in our preliminary patient data, only DF analysis allows to identify the atrial drivers.

5. Conclusion

Identification of atrial sources by solving the inverse problem of the electrocardiography is more reliably accomplished in the frequency domain than based on PS detection.

Acknowledgements

Supported in part by: Instituto de Salud Carlos III (Ministry of Economy and Competitiveness, Spain: PI13-00903, PI14/00857) and Spanish Society of Cardiology (Grant for Clinical Research in Cardiology 2015).

References

[1] Cappato R, Calkins H, Chen SA, Davies W, Iesaka Y, Kalman J, Kim YH, Klein G, Natale A, Packer D, Skanes A, Ambrogi F, Biganzoli E. Updated worldwide survey on the methods, efficacy, and safety of catheter ablation for human atrial fibrillation. Circ Arrhythm Electrophysiol. 2010;3:32-8.

[2] Tzou WS, Marchlinski FE, Zado ES, Lin D, Dixit S, Callans DJ, Cooper JM, Bala R, Garcia F, Hutchinson MD, Riley MP, Verdino R, Gerstenfeld EP. Long-term outcome after successful catheter ablation of atrial fibrillation. Circ Arrhythm Electrophysiol. 2010;3:237-42.

[3] Chao TF, Tsao HM, Lin YJ, Tsai CF, Lin WS, Chang SL, Lo LW, Hu YF, Tuan TC, Suenari K, Li CH, Hartono B, Chang HY, Ambrose K, Wu TJ, Chen SA. Clinical outcome of catheter ablation in patients with nonparoxysmal atrial fibrillation: Results of 3-year follow-up. Circ Arrhythm Electrophysiol. 2012;5:514-20.

[4] Narayan SM, Krummen DE, Shivkumar K, Clopton P, Rappel WJ, Miller JM. Treatment of atrial fibrillation by the ablation of localized sources: Confirm (conventional ablation for atrial fibrillation with or without focal impulse and rotor modulation) trial. Journal of the American College of Cardiology. 2012;60:628-36

[5] Haissaguerre M, Hocini M, Denis A, Shah AJ, Komatsu Y, Yamashita S, Daly M, Amraoui S, Zellerhoff S, Picat MQ1, Quotb A, Jesel L, Lim H, Ploux S, Bordachar P, Attuel G, Meillet V, Ritter P, Derval N, Sacher F, Bernus O, Cochet H1, Jais P, Dubois R. Driver domains in persistent atrial fibrillation. Circulation. 2014;130:530-8.

[6] Dössel O, Krueger MW, Weber FM, Wilhelms M, Seemann G. Computational modeling of the human atrial anatomy and electrophysiology. Med. Biol. Eng. Comput. 2012;50:773-9.

[7] Koivumäki JT, Seemann G, Maleckar MM, Tavi P. In silico screening of the key cellular remodeling targets in chronic atrial fibrillation. PLoS Comput Biol. 2014;10:e1003620.

[8] Atienza F, Almendral J, Moreno J, Vaidyanathan R, Talkachou A, Kalifa J, Arenal A, Villacastin JP, Torrecilla EG, Sanchez A, Ploutz-Snyder R, Jalife J, Berenfeld O. Activation of inward rectifier potassium channels accelerates atrial fibrillation in humans: Evidence for a reentrant mechanism. Circulation. 2006;114:2434-44.

[9] Garcia V, Liberos A, Vidal AM, Guillem MS, Millet J, González A, Martinez-Zaldivar FJ, Climent AM. Adaptive step ODE algorithms for the 3D simulation of electric heart. Comput Biol Med. 2014;44:15-26.

[10] Rodrigo M, Guillem MS, Climent AM, Pedron-Torrecilla J, Liberos A, Millet J, Fernandez-Aviles F, Atienza F, Berenfeld O. Body surface localization of left and right atrial high-frequency rotors in atrial fibrillation patients: A clinical-computational study. Heart Rhythm. 2014;11:1584-91.

[11] Pedrón-Torrecilla J, et al. Noninvasive Estimation of Epicardial Dominant High-Frequency Regions During Atrial Fibrillation. J Cardiovasc Electrophysiol. 2016;27:435-42.

[12] Guillem MS, Climent AM, Millet J, Arenal A, Fernandez-Aviles F, Jalife J, Atienza F, Berenfeld O. Noninvasive localization of maximal frequency sites of atrial fibrillation by body surface potential mapping. Circulation. Arrhythmia and electrophysiology. 2013;6:294-301

[13] Zlochiver S, Yamazaki M, Kalifa J, Berenfeld O. Rotor meandering contributes to irregularity in electrograms during atrial fibrillation. Heart Rhythm 2008;5:846–54.

Address for correspondence.

María S Guillem
ITACA. Edificio 8G acceso B. Universitat Politécnica de València. Camino de Vera s/n. 46022 Valencia, Spain
mguisan@itaca.upv.es